through the glass section of the column. Also, to save time, the 10.2 cm ID column (with the 1 mm 4-hole distributor) which was in operation at that time was used. Since there was not enough catalyst to load this large column, we used a relatively low (2 wt %) catalyst loading The liquid medium was spent Run CT-256-8 slurry diluted wih the same wax. The gas holdup at 260°C and 0-6 cm/s superficial gas velocities was about 9% lower than that given by the same reactor-wax without any catalyst. The trend of lower gas holdup due to the presence of solids is consistent with literature findings.

F. Evaluation of Continuous Stirred-Tank Reactors Using Mathematical Models

In a search for slurry F-T reactor designs that may give better performance than bubble-column (BC) reactors, continuous stirred-tank reactors (CSTR's) in series were investigated using mathematical models. A series of CSTR's has several potential advantages over BC reactors:

- Higher catalyst loading.
- Reduced gas-liquid interphase mass-transfer resistances.
- Established scale-up experience.

Possible disadvantages of series of CSTR's are gas and liquid-phase backmixing, and increased capital and operating cost due to power requirements for stirring.

In this work the effect of the gas and liquid-phase backmixing and the elimination of the mass-transfer resistances was investigated using a multi-component mathematical model for a series of slurry CSTR's. The results were compared with predictions of the BC multi-component model (Kuo, 1983). The base conditions of all calculations are: I-B catalyst, 260°C, 2.14 MPa, 25 wt % catalyst loading, 0.7 feed H_2/CO ratio and 86 mol % H_2+CO conversion. The major highlights from the calculations are:

- The benefit of reducing the mass-transfer resistances by using a CSTR system is rather minor because the gas-liquid interphase mass-transfer resistances in the bubble-column base case is small.
- The major penalty of a CSTR system is the gas- and liquid-phase backmixing which results in a reduction of the H_2 and CO partial pressures. The extent of this penalty can be reduced, as indicated by a decrease in the total reactor volume, by increasing the number of CSTR's in series.

- By increasing the number of CSTR's in series, it is possible to have a total reactor volume less than that of a single bubble-column reactor to achieve the same conversion. In this case study, the crossover point is seven CSTR's in series.

The major potential benefits of using CSTR over BC is probably the increase in catalyst loading. The limiting factor may very well be the catalyst settling phenomenon enountered in many of our bubble-column runs (see Chapter IV). The catalyst loading may be one of the process variables that influence the operating time period before catalyst settling takes place. Use of CSTR's may provide the mechanical agitation that will prevent or delay this settling. Experiments are needed to evaluate this possibility.

To evaluate the CSTR's advantage of reducing the gas-liquid interphase mass-transfer resistance over the BC's, the quantification of this resistance in the base BC case is essential. An improved mathematical model of a "series of cells" concept that is applicable to both BC and CSTR was adopted for this study. However, after using two different approaches in an attempt to establish this base case resistance, we could only conclude qualitatively that this resistance may be quite small in three BC cases. Furthermore, one cannot establish the power requirement for CSTR without establishing the gas-liquid interphase mass-transfer resistance in the base BC case.

F.1. Description of a CSTR Mathematical Model

Except for the perfect mixing in the gas- and liquid-phase, the major assumptions are similar to those used for the BC multi-component model (Kuo, 1983):

- Mass transfer resistances to H_2, CO, CO_2, and H_2O diffusion at the liquid side of the gas-liquid interface.
- Two consecutive reactions:

  Fischer-Tropsch:

$$CO + (1+m/2)\ H_2 = (-CH_m) + H_2O \qquad \text{(VII-15)}$$

$$r_1 = k_1[H_2][CO]/([CO] + k_3[H_2O]) \qquad \text{(VII-16)}$$

  Water-Gas Shift:

$$CO + H_2O = CO_2 + H_2 \qquad \text{(VII-17)}$$

$$r_2 = k_2([CO][H_2O]-[H_2][CO_2]/k_4)/([CO]+k_3[H_2O]) \quad \text{(VII-18)}$$

- Molar contraction due to synthesis reaction is a linear function of synthesis gas conversion.
- Constant bubble-size and gas holdup.
- Steady-state isothermal and isobaric operation.
- Perfectly mixed gas- and liquid-phase.

Material balances for the gas- and liquid-phase of the components H_2, CO, CO_2 and H_2O (denoted by subscripts 1, 2, 3, 4, respectively), yield:

$$Q^i C_{gi}{}^i - Q^e C_{gi}{}^e = k_{Li} a_g (C_{gi}{}^e/K_i - C_{Li}) V/N, \; i = 1,\ldots,4 \quad \text{(VII-19)}$$

for the gas-phase, and

$$k_{Li} a_g (C_{Li} - C_{gi}{}^e/K_i) = (1-\epsilon_g)(1-v_c) C_{Fej} \sum_j S_{ij} r_j, \; i = 1,\ldots,4 \quad \text{(VII-20)}$$

for the liquid-phase, where r_1 and r_2 are respectively, the F-T and the water-gas shift reaction rates given by Equations (VII-16) and (VII-18), and S_{ij} ($i = 1,\ldots,4$; and $j = 1,2$) are elements of the stoichiometric matrix.

Assuming that the molar contraction due to the F-T reaction is linear with respect to the H_2+CO conversion, the following relation between the gas flow rate and the H_2+CO conversion was obtained:

$$Q^e = Q^i(1 + \alpha X_{H_2+CO}) \quad \text{(VII-21)}$$

where α is the constant molar contraction factor.

In dimensionless form, Equations (VII-19) to (VII-21) become:

$$\bar{Q}\bar{C}_{gi}{}^e - \bar{C}_{gi}{}^i + St_{di}(\bar{C}_{gi}{}^e - \bar{C}_{Li}) = 0 \quad \text{(VII-22)}$$

$$St_{di}(\bar{C}_{gi}^{e} - \bar{C}_{Li}) + \sum_j S_{ij} St_{kj} \bar{r}_j = 0 \qquad \text{(VII-23)}$$

for $i = 1,\ldots,4$

A solution for this set of non-linear algebraic equations can be obtained using a conventional Newton-Raphson iteration routine. The convergence criterion of the iterative scheme is that the successive approximations for the dependent variables be within 0.1% of each other. The calculation procedure for a series of CSTR's is as follows:

1. Choose a total reactor volume, V, and a number of CSTR's, N.

2. Solve Equations (VII-22)-(VII-23) for the first CSTR.

3. Use output from each CSTR as input to the next, and solve Equations (VII-22)-(VII-23) for remaining CSTR's.

In a mechanically agitated slurry reactor, the hydrodynamics can be controlled independently of the gas throughput by varying the stirring speed. Increasing the stirring speed increases the gas-liquid interfacial area and this decreases the mass transfer resistance (e.g. Joshi et al., 1982). At sufficiently high stirring speeds, the mass transfer resistance becomes negligible and equilibrium is achieved between the bulk gas and the gas absorbed in the liquid. This special case of no mass transfer resistance can be described by the following dimensionless material balance equations:

$$\bar{C}_{gi}^{e} = \bar{C}_{Li} \qquad \text{(VII-24)}$$

$$\bar{Q}\bar{C}_{gi}^{e} - \bar{C}_{gi}^{i} = \sum_j S_{ij} St_{kj} \bar{r}_j \qquad \text{(VII-25)}$$

for $i = 1,\ldots,4$

The solution procedure and convergence criteria for Equations (VII-24)-(VII-25) are identical to those of Equations (VII-22)-(VII-23) described above.

F.2. Use of a Series of CSTR's to Compensate the Penalty Due to Backmixing in BC

The correlations used to estimate the model parameters are the same as those in Tables 27 and 28 in the Final Report of our earlier Contract (Kuo ,1983). The kinetic constants k_1, k_2, k_3, and k_4 were estimated from the two-stage pilot plant data (Section VII.E in Kuo, 1983) and are given again in Table VII-11, together with other pertinent parameters used in the calculations. Note that the same gas holdup correlation developed by Deckwer et al. (1980) for a bubble-column (Table 27 in Kuo, 1983), is also used to predict the gas holdup in the CSTR model. The assumption is that for the same gas throughput, there is a stirrer speed for which each gas holdup (or higher) can be achieved in the CSTR.

Figure VII-45 shows the effect of mass-transfer resistance on H_2+CO conversion. For a series of five CSTR's at the base conditions, there is little gain in eliminating the mass-transfer resistance. Note that this result is only valid at the base conditions in which the gas-liquid interphase mass-transfer resistance for the BC is very small.

In Figure VII-46, series of CSTR's with no mass transfer resistances are compared at base conditions with a single BC reactor. Increasing the number of reactors in a CSTR system decreases the conversion difference between the BC system and the CSTR system due to the reduction of the gas- and liquid-phase backmixing. Thus, a system of three CSTR's requires only about a 10% larger reactor volume to achieve 86 mol % H_2+CO conversion than the BC case; two and one CSTR's require 20 and 80% larger volumes, respectively, than the BC. Calculations show that seven or more CSTR's require a slightly less reactor volume than a BC to achieve 86 mol % H_2+CO conversion.

F.3. An Improved Mathematical Model for Both CSTR and Bubble-Column

A "series of cells" concept was used to construct a reactor model that is applicable to both CSTR and BC. The use of this model for CSTR is straight forward and is similar to what was described in the Subsection VII.F.1. This model can also be used for bubble-columns if a number of cells can be predetermined to simulate the axial dispersion in the bubble-columns. Such a relation is obtained by assuming identical standard deviations of the residence time distribution functions for a series of homogeneous cells and a homogeneous axially mixed column (Levenspiel, 1979):

$$N = 0.5\ Pe_L/(1-(1-\exp(-Pe_L))/Pe_L) \qquad \text{(VII-26)}$$

Table VII-11

Parameters Used in Fischer-Tropsch CSTR Mathematics Model Calculations

	Base
T, °C	260
P, MPa	1.48
u_g^i, cm/s(1)	4
w_c, wt %	15
f	0.7
m	2.24
k_1, cm^3 liquid/gFe-s	0.50
k_2, cm^3 liquid/gFe-s	1.35
k_3	0.20
k_4	37.5

(1)Used only for the bubble-column base case calculation.

Figure VII-45

EFFECT OF MASS TRANSFER RESISTANCE ON CONVERSION FOR A SERIES OF CSTR'S

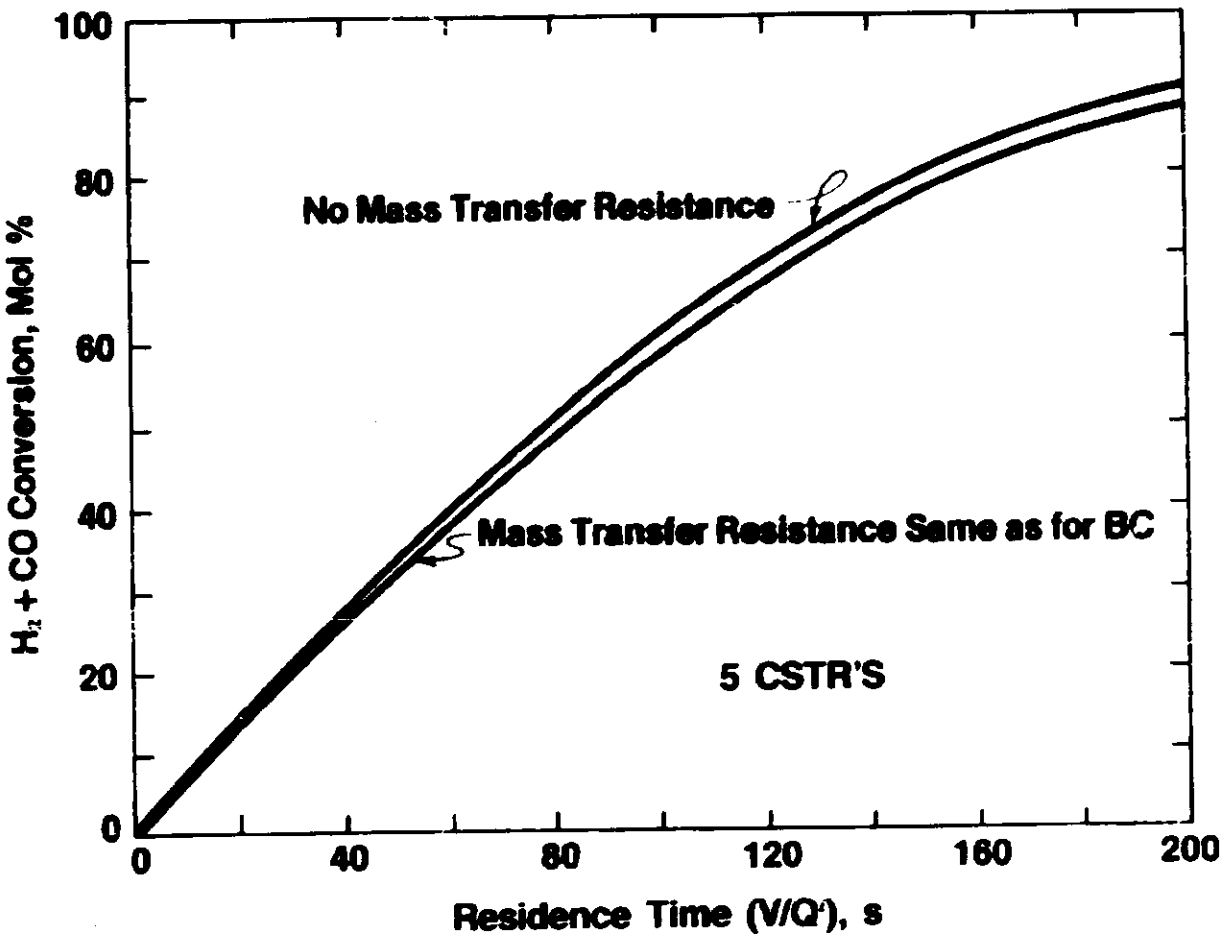

Figure VII-46

COMPARISON OF BC AND SERIES OF CSTR'S

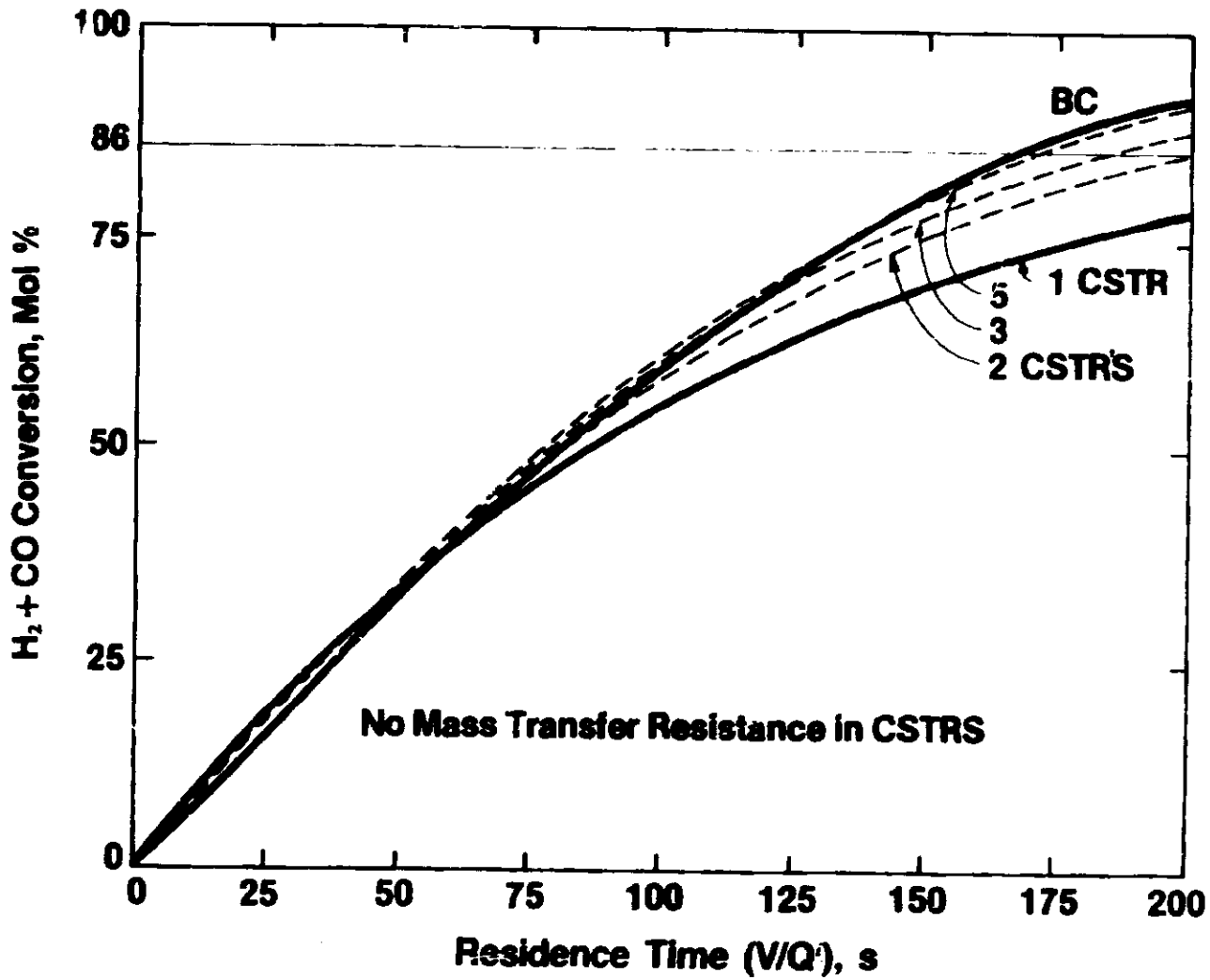

where Pe_L, the liquid-phase Peclet number, is directly related to the liquid-phase axial dispersion coefficient. In the current studies, a correlation on this coefficient reported by Shah and Deckwer (1985) is used.

The following improved rate expressions for both F-T and water-gas shift reaction were also adopted here:

$$r_1 = k_1[H_2][CO]/([CO]+k_1'[CO_2]+k_1''[H_2O]) \qquad \text{(VII-27)}$$

$$r_2 = k_2'([CO][H_2O]-[H_2][CO_2]/k_4)/ ([CO]+k_1'[CO_2]+k_1''[H_2O])^2 \qquad \text{(VII-28)}$$

These two expressions replace the Equations (VII-16) and (VII-18) mentioned earlier. Both expressions include CO_2 inhibition in addition to H_2O inhibition used earlier. Deckwer et al. (1984) showed that this term is essential when there is substantial CO_2 present. The denominator is consistent with an Elly-Rideal mechanism, obtained when an enolic polymerization mechanism is assumed for the F-T reactions. The water-gas shift reaction rate expression has a denominator consistent with a Langmuir-Hinshelwood mechanism, and was recommended by Podolski (1974).

F.4. Bubble-Column Versus CSTR: Evaluation of the Gas-Liquid Interphase Mass-Transfer Resistance

To compare CSTR with BC, an establishment of the gas-liquid interphase mass-transfer resistance for the BC is needed for both high-wax and low-wax mode operations. We adopted two approaches to evaluate this resistance. In the first approach, we used the literature correlations, while in the second approach we tried to back-calculate this resistance using intrinsic kinetics estimates from autoclave data which we expect to contain little mass-transfer resistance.

In the first approach, the gas holdup, bubble size, and the mass-transfer coefficients were estimated from literature correlations of Miller (1974) and Lehrer (1971). These correlations include the effect of mechanical agitation (for CSTR) as well as gas sparging (for BC). Since we are trying to compare these two reactors, we felt that it was necessary to use the hydrodynamic correlations applicable to both systems. The major assumption in these correlations is that hydrodynamic parameters are a function of the total power input per unit volume. The total power input is a linear combination of the mechanical power input and the power input by gas sparging.

These correlations, however, were developed based on data from non-Fischer-Tropsch and non-commercial scale systems. Its application to the present system is highly questionable. Nevertheless, the attempt given here is our best effort in estimating the mass-transfer resistance from literature data. Using these correlations, the bubble size in the BC was estimated to be 7.6 mm, which was substantially higher than the 0.7 mm assumed previously. The larger bubble size, of course, gave very low specific surface area and subsequently high mass-transfer resistance for the bubble-column case. The mass-transfer resistance in a CSTR was negligible. The comparison of the performances of a bubble-column (with 25% catalyst loading) and a series of three CSTRs (with 35% of catalyst loading) using the mathematical model described in the preceding Subsection showed that up to 100% increase in throughput can be achieved in the CSTRs due partly to reduced mass transfer resistance by mechanical agitation.

We feel that the gas-liquid interphase mass-transfer resistance estimated from these correlations probably provides the upper-bound of the mass-transfer resistance in a slurry F-T bubble-column.

In a second approach, we attempted to back-calculate the mass-transfer resistance in the Rheinpreussen demonstration reactor and Koelbel's laboratory scale unit (Koelbel et al., 1955), and our two-stage BSU by using a known intrinsic kinetics. To obtain the intrinsic kinetics for a K-promoted co-precipitated Fe catalyst, we used the autoclave data of Ledakowicz et al. (1985). Assuming mixed gas and liquid phases and negligible mass-transfer resistance, the intrinsic kinetic constants k_1 and k_2' were estimated by best fit of H_2 and CO conversions for each data point in the data base covering a H_2+CO conversion range of 20-88 mol %. The water-gas shift reaction was found to be very close to equilibrium corresponding to an expected high shift activity of this K-promoted catalyst. However, the F-T kinetic constant k_1 was found to increase greatly with the data of increasing H_2+CO conversion. Figure VII-47 is a plot of k_1 as a function of H_2+CO conversion for the data set used to estimate k_1. The value of k_1 reported here is adjusted to the base case temperature of 260°C by assuming an activation energy of 100 kJ/mol. The data base covered a temperature range of 220-260°C.

As shown in the figure, the k_1 varies from 0.38 to 2.67 cm^3-liquid/s-gFe with a conversion range of 20 to 88 mol %. A similar variation on k_1 was also obtained when we used the Mobil's proprietary autoclave data. This wide spread on the estimated kinetic constant indicates two deficiencies. The first is the inadequacy of the existing kinetic mechanism to cover a wide range of conversions. The other is that the estimated

Figure VII-47
ESTIMATED INTRINSIC F-T KINETIC CONSTANT

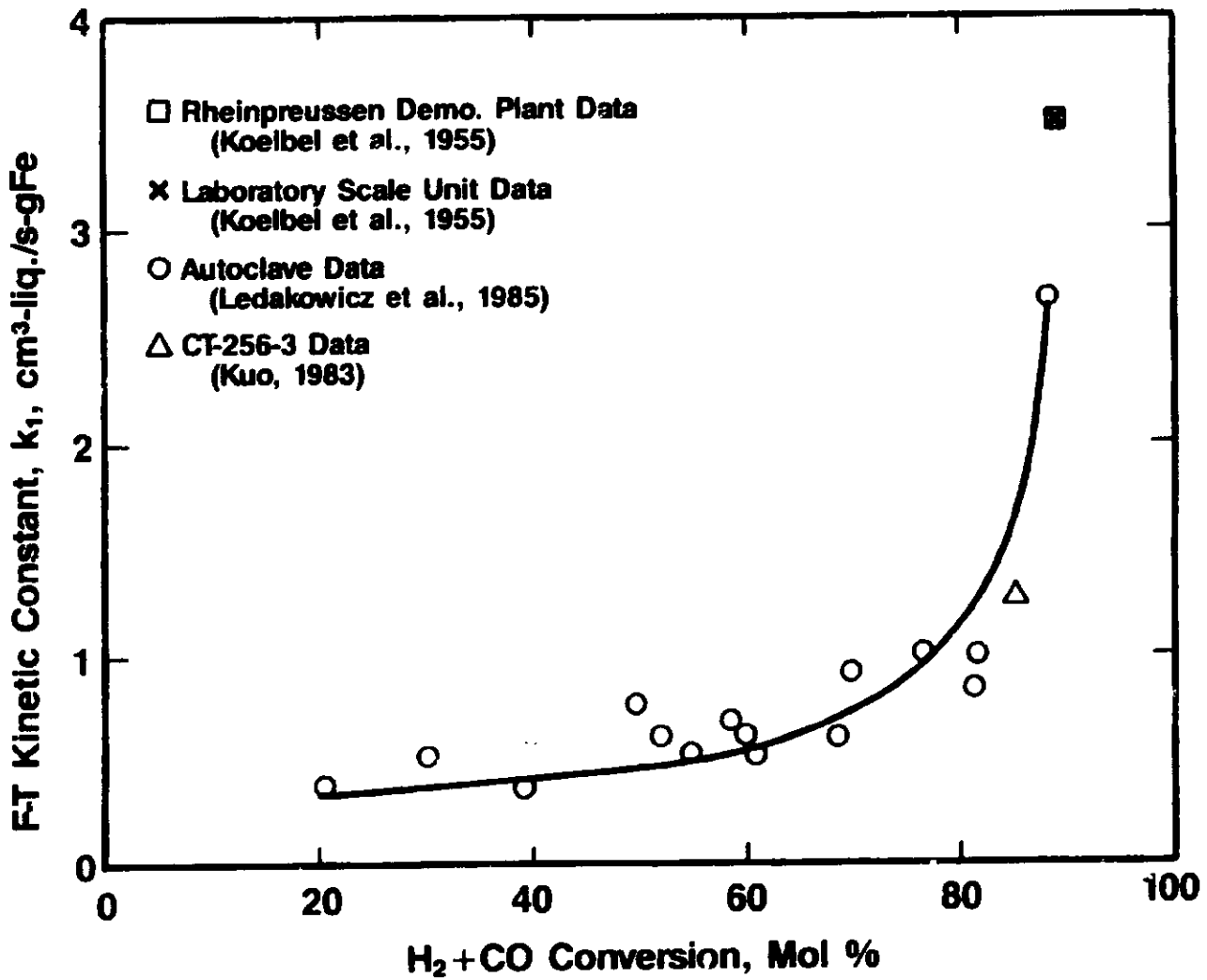

kinetic constant is highly sensitive with respect to the data base used. Consequently, it is impractical to back-calculate the mass-transfer resistance in a bubble-column reactor using the estimated intrinsic kinetic constant.

A related effort is to estimate the intrinsic kinetic constants from the bubble-column data assuming negligible mass-transfer resistance and then compare them with those estimated from the autoclave data at the similar conversion. Both data from the Rheinpreussen demonstration reactor (Koelbel et al., 1955) and a bench-scale unit of Koelbel et al. (1955) gave k_1 and k_2' values of 3.5 cm^3-liquid/s-gFe and 17.1 x 10^{-5} mol/s-gFe. It should be again pointed out here that the estimated kinetic constant k_1 is extremely sensitive to the H_2+CO conversion level of the data set. For example, a value of k_1 between 2.3 and 4.6 can fit the H_2+CO conversion within 1 mol %. Thus, comparing the k_1 value obtained from data of Koelbel et al., with the estimated k_1 from the autoclave data, we can qualitatively conclude that the bubble-column mass-transfer resistance may be quite small. Similar conclusion can be drawn from our bubble-column data from CT-256-3 run (Kuo, 1983). These estimated k's are also plotted in Figure VII-47.

In conclusion, we strongly recommend direct measurement of the gas-liquid interphase mass-transfer resistance in F-T bubble-columns.

VIII. Task 5 - Development of Conceptual Process Schemes

A. Introduction

A conceptual process design and scoping cost estimate for a commercial plant producing 30,731 BPSD of G+D has been developed for the two-stage slurry F-T/ZSM-5 process. The objectives of the study are two-fold. One is to study the layout of all the processing units and equipment; the other is to provide guidances for future research and development. The design of the plant is a battery limit part of a complete coal conversion complex. The feed to this plant is a clean synthesis gas derived from a BGC (British Gas Corporation)/Lurgi slagging gasifier which is not included in this design and cost estimate. The composition and quantity of the feed-gas to the first-stage F-T reactors are those used in an earlier study (Kuo, 1983). They are also the same as those in a report by Gray et al. (1980).

In order to minimize methane + ethane yield and maximize liquid fuel (gasoline and distillate) yields, it is necessary to increase reactor-wax yields from the first-stage F-T reactor. For instance, in the previous contract work (Kuo, 1983) we showed that when the methane + ethane yield dropped from 10 wt % of the total hydrocarbons produced to 4 wt %, the reactor-wax yield increased from 8 to 50 wt %. A further drop of the methane + ethane yield to 2 wt % increased the wax yield to 80 wt %. Hence, in the high wax (low methane + ethane) operation mode, it is essential to convert efficiently the reactor-wax into high quality fuels. In the Appendix-Restrictive Distribution, we described some scoping studies to upgrade reactor-wax into gasoline and distillate products. The results of these studies are incorporated in the conceptual design.

To maintain a reasonable G/D product ratio and sufficiently low methane + ethane yield, we set a target reactor-wax of 50 wt % with a corresponding methane + ethane yield of 4 wt %. The material balance #10 of Run CT-256-7 was chosen as a basis for F-T process data. The balance gave a reactor-wax yield of 57 wt % and a methane + ethane yield of 3.8 wt %, at 81 mol % H_2+CO conversion. These data were adjusted slightly to give the target methane + ethane reactor-wax yields. The target H_2+CO conversion was 84 mol % (corresponding to 90% CO conversion). Unfortunately, detailed analysis of the overhead C_5^+ F-T product of Run 7 was not available. To fill this gap, the hydrocarbon distribution of the same stream used to develop the design base case data of our previous contract (Kuo, 1983) was used. Based on our experience, the C_5^+ hydrocarbon

distributions in the overhead of the slurry F-T reactor changed only slightly with the process conditions. The ZSM-5 reactor data is based on material balance #14 of Run CT-256-7, which had a severity index (molar isobutane/(butenes + propene) ratio) of .73. This data was adjusted to give the same severity as that in the previous contract (.78). All material balance data were slightly adjusted to give exact C-H-O balances.

The reactor-wax upgrading to gasoline and distillate is based on our scoping studies using Run CT-256-4 reactor-wax. Runs CT-256-4 and -7 both used the same F-T Catalyst I-B at the same reaction conditions, and produced similar hydrocarbon selectivities. Thus, the reactor-waxes produced in these runs are also expected to have similar compositions. A detailed carbon number distribution of Run CT-256-4 reactor-wax is available up to C_{55} by GC, and the C_{55}^{+} content is known from FIMS analysis.

Two reactor-wax upgrading schemes are included in the conceptual design and are described in the Appendix-Restrictive Distribution.

B. Design Base Data For Slurry Fischer-Tropsch/ZSM-5 Unit

The operating conditions of the slurry F-T and ZSM-5 reactors are summarized in Table VIII-1. The heats of reaction and adiabatic temperature rise were estimated. The space velocity for the ZSM-5 reactor was estimated from that of the previous contract, assuming the same contact time. The space velocity of the F-T reactor was estimated from that of the previous contract, but we allowed a 15% drop due to a slight pressure effect, i.e., higher pressure at the same superficial gas velocity will somewhat reduce the H_2+CO conversion.

Tables VIII-2 and -3 show product yields for F-T and ZSM-5 reactors, as mol/100 mol feed H_2+CO. Table VIII-2 also includes the feed H_2, CO, and H_2O to the F-T reactor. We assume that the water-gas shift reaction will convert rapidly the excess CO and water into H_2 and CO_2, to give an effective H_2/CO ratio of 0.67.

For convenience, the slurry F-T operation conditions and product breakdowns for the present design base as well as those for the gasoline model design base used in the earlier Contract (Kuo, 1983) are summarized in Appendix I. The current design base data were adopted earlier in the contract work and therefore are somewhat different from those of Run CT-256-13 (see Section IV.L), the best high-wax mode operation demonstrated during this Contract. For comparison, the typical conditions and product breakdowns of this run are also included in Appendix I.

Table VIII-1

Slurry Fischer-Tropsch/ZSM-5
Process Conditions

	First-Stage (F-T)	Second-Stage (ZSM-5)
Catalyst	I-B(Pptd Fe/Cu/K_2CO_3)	ZSM-5
Feed H_2/CO, molar	0.5	-
Inlet Pres., MPa	2.87 (402 psig)	Cascaded
Inlet Temp., °C	227	371
Outlet Temp., °C	258	393
Space Velocity	3.50 NL(H_2+CO)/gFe-hr	8.0 NL/gCat-hr
Heat of Reaction, kJ/mol Feed H_2+CO	56.3	0.6

Table VIII 2
FIRST STAGE PRODUCT YIELDS
(BASIS: 100 MOL FEED H2-CO)

	FEED MOLES	MW	SP GR	MOLES
WATER	6.7864	18.02		0.7902
HYDROGEN	33.3333	2.02		9.9537
CO	66.6667	28.01		5.9880
CO2		44.01		33.1333
METHANE		16.04		0.8249
ETHENE		28.05		0.2611
ETHANE		30.07		0.0875
PROPENE		42.08	0.5218	0.2615
PROPANE		44.10	0.5077	0.0688
N-BUTANE		58.12	0.5832	0.0648
C4 OLEFINS		56.11	0.6011	0.1731
N-PENTANE		72.15	0.6306	0.0694
C5 OLEFINS		70.14	0.6471	0.2291
N-HEXANE		86.18	0.6641	0.0586
C6 OLEFINS		84.16	0.6781	0.1517
N-HEPTANE		100.11	0.6886	0.0314
C7-OLEFINS		98.19	0.7026	0.0766
N-OCTANE		114.23	0.7067	0.0343
C8-OLEFINS		112.21	0.7201	0.0721
N-NONANE		128.26	0.7179	0.0318
C9-OLEFINS		126.24	0.7339	0.0565
C10-C15 (P+O)		167.82	0.7572	0.2278
C16-C20 (P+O)		245.95	0.7861	0.0538
C21-C25 (P+O)		311.75	0.7994	0.0092
C26+ (P+O, EXCL. WAX)		384.55	0.8101	0.0007
METHANOL		32.04	0.7960	0.0413
FORMIC ACID		46.03	1.2210	0.0022
ETHANOL		46.07	0.7900	0.0855
ACETIC ACID		60.05	1.0500	0.0055
ACETONE		58.08	0.7920	0.0144
N-PROPANOL		60.10	0.8050	0.0425
I-PROPANOL		10	0.7900	0.0098
PROPANOIC ACIDS		8	0.9930	0.0021
C4-C9 (OXYGENATES)			0.8248	0.0721
C10-C15 (OXYGENATES)			0.8471	0.0164
C16-C20 (OXYGENATES)		2[illegible]	0.8472	0.0017
C21-C25 (OXYGENATES)		330.75	0.8460	0.0000
C26+ (OXYGENATES)		417.58	0.8450	0.0000
REACTOR WAX		821.41	0.8700	0.2414
TOTAL MOLES	106.7864			53.2448
TOTAL WT	2056.80			2056.80
HYDROCARBON WT				396.5330

Table VIII-3

SECOND-STAGE PRODUCT YIELDS

(BASIS 100 MOL FEED H2+CO)

	MW	SP.GR	MOLES
WATER	18.02	-	1.0977
HYDROGEN	2.02	-	9.9537
CO	28.01	-	6.9888
CO2	44.01	-	33.1334
METHANE	16.04	-	0.8434
ETHANE	30.07	-	0.0923
ETHENE	28.05	-	0.1561
PROPANE	44.10	0.5077	0.2836
PROPENE	42.08	0.5218	0.1617
N-BUTANE	58.12	0.5844	0.1860
I-BUTANE	58.12	0.5631	0.2365
N-BUTENE	56.11	0.6011	0.0866
I-BUTENE	56.11	0.6100	0.0577
N-PENTANE	72.15	0.6312	0.1134
I-PENTANE	72.15	0.6248	0.1960
N-PENTENE	70.14	0.6461	0.0845
T-PENTENE	70.14	0.6326	0.1236
CYCLOPENTANE	70.14	0.7505	0.0043
N-HEXANE	86.18	0.6640	0.2624
I-HEXANE	86.18	0.6579	0.1144
N-HEXENE	84.16	0.6786	0.0010
I-HEXENE	84.16	0.6722	0.0273
METHYLCYCLOPENTANE	84.16	0.7505	0.0254
CYCLOHEXANE	84.16	0.7834	0.0010
BENZENE	78.11	0.8845	0.0114
N-HEPTANE	100.21	0.6882	0.0305
I-HEPTANE	100.21	0.6838	0.0538
N-HEPTENE	98.19	0.7058	0.0273
I-HEPTENE	98.19	0.6992	0.0061
DIMETHYL-CYCLOPENTANE	98.19	0.7406	0.0221
METHYLCYCLOHEXANE	98.19	0.7748	0.0123
TOLUENE	92.14	0.8719	0.0447
N-OCTANE	114.23	0.7068	0.0149
I-OCTANE	114.23	0.7090	0.0249
N-OCTENE	112.21	0.7272	0.0289
I-OCTENE	112.21	0.7180	0.0085
C8-N6	112.21	0.7729	0.0225
C8-N8	112.21	0.7841	0.0126
P-XYLENE	106.17	0.8657	0.0148
M-XYLENE	106.17	0.8687	0.0471
O-XYLENE	106.17	0.8848	0.0153
ETHYLBENZENE	106.17	0.8717	0.0175
N-NONANE	128.26	0.7178	0.0057
I-NONANE	128.26	0.7258	0.0129
N-NONENE	126.24	0.7369	0.0162
I-NONENE	126.24	0.7385	0.0038
C9-N6	126.24	0.7848	0.0084
C9-N8	126.24	0.7945	0.0047
N-PROPYLBENZENE	120.20	0.8666	0.0038
I-PROPYLBENZENE	120.20	0.8690	0.0067
METHYL-ETHYL-BENZENE	120.20	0.8696	0.0530
TRIMETHYL-BENZENE	120.20	0.7340	0.0250
N-DECANE	142.28	0.7451	0.0015
N-C4-BENZENE	134.22	0.7493	0.0107
METHYL [illegible]-C3-BENZENE	134.22	0.7954	0.0029
TETRA [illegible]ETHYL-BENZENE	134.22	0.8078	0.0031
DIETHYLBENZENE	134.22	0.8700	0.0171
C11-ALKYLBENZENE	148.25	0.8800	0.0050
C12-PARAFFIN	170.34	0.7526	0.0034
C12-ALKYLBENZENE	161.2.	0.8617	0.0061
C13-PARAFFIN	184.37	0.7661	0.0027
C13-ALKYLBENZENE	176.30	0.8609	0.0050
C14-PARAFFIN	198.39	0.7667	0.0015
C14-ALKYLBENZENE	190.33	0.8603	0.0036
TOTAL MOLES			53.6667
TOTAL WT			1868.54
HYDROCARBON WT			198.273

The major difference on operation conditions is the lower pressure (1.38 versus 2.45 MPa in H_2-CO pressure) used in Run CT-256-13. In a scoping economic sensitivity study, we found that a decrease in the operating pressure of the slurry F-T reactor section results in:

- An elimination of the feed-gas compressor.
- An increase in steam export.
- A decrease in the material cost for the reactor section.
- A decrease in the height of slurry F-T reactors with a corresponding increase in the total number of reactors.

We expect an overall decrease of 2-5% of the investment cost may result from this change. The methane + ethane selectivity is also somewhat lower which shall result in higher liquid fuel yield.

C. Conceptual Process Schemes

For convenience, the conventional engineering units are used throughout this section.

C.1. Conceptual Process Design

C.1a. Feed Gas Basis

The synthesis gas used as feed is obtained by gasification of Wyoming subbituminous coal in advanced type gasifiers such as the BGC/LURGI slagger. The synthesis gas is treated to remove sulfur and carbon dioxide prior to feeding the slurry F-T reactor.

The clean synthesis gas is assumed available at 350 psig and 100°F from the coal gasification complex and is compressed within the battery limits. The feed rate and composition of the synthesis gas are as follows:

	Lb-mol/hr	Mol %
H_2	31,853	29.83
CH_4	7,496	7.02
CO	64,347	60.26
CO_2	2,360	2.21
N_2	363	0.34
C_2H_4	21	0.02
C_2H_6	342	0.32
Total Lb-mol/hr	106,782	100.00
Total Lb/hr	2,111,070	

To raise the H_2/CO ratio of the synthesis gas, a stoichiometric amount of steam is added to the feed in order to promote water-gas shift reaction and raise the ratio to 0.67 which is the value used in the laboratory experiments of the two-stage process. The assumption that the shift reaction takes place at the slurry F-T reactor without affecting the slurry F-T catalyst activity is supported by Koelbel a . lek (1980) and in-house Mobil research work.

C.1b. Process Flow Dia

Figure VIII-1 shows the slu -5 reactors and the F-T reactor-wax/catalyst separation, and igure VIII-2 shows the process flow diagram for the slurry F-T catalyst preparation and pretreatment.

Figure VIII-3 shows the plan arrangement of the slurry F-T/ZSM-5 reactor section. Other process flow diagrams, including the F-T reactor-wax upgrading and product distillation are given in the Appendix-Restrictive Distribution.

C.1c. Overall M rial Balances and Pro Qualities

Overall material bal s and product qualities are included in the Appendix-Restrictive Distribution.

C.2. Plant Description

The plant consists essentially of three main sections; the slurry F-T/ZSM-5 reactor section, the F-T reactor-wax upgrading section and the product recovery section.

The reacto section encompasses the slurry F-T and ZSM-5 reactors plus the auxiliary facilities to prepare and pretreat the F-T catalyst and to regenerate the ZSM-5 catalyst.

The reactor-wax upgrading section contains the facilities to clean up the wax product from F-T catalyst fines and also the process units necessary to convert the clean reactor-wax into G+D products. The description of this section is given in the Appendix-Restrictive Distribution.

The product recovery section is a conventional distillation train designed to maximize C_3 and C_4 recovery and to produce products with proper specification.

Figure VIII-1

SLURRY FISCHER-TROPSCH/ZSM-5 REACTORS AND REACTOR-WAX SEPARATION

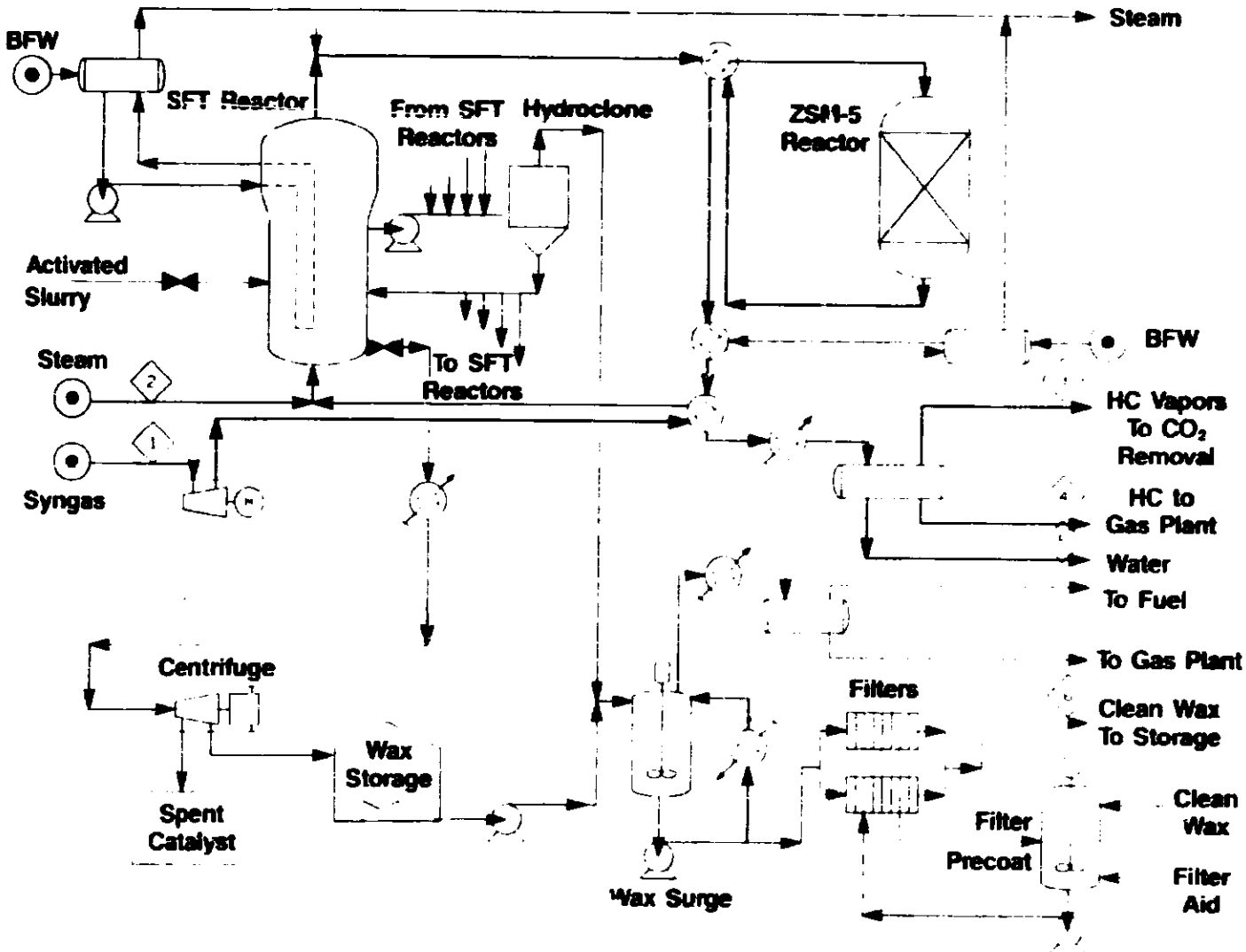

Figure VIII-2

SLURRY FISCHER-TROPSCH CATALYST PRETREATMENT

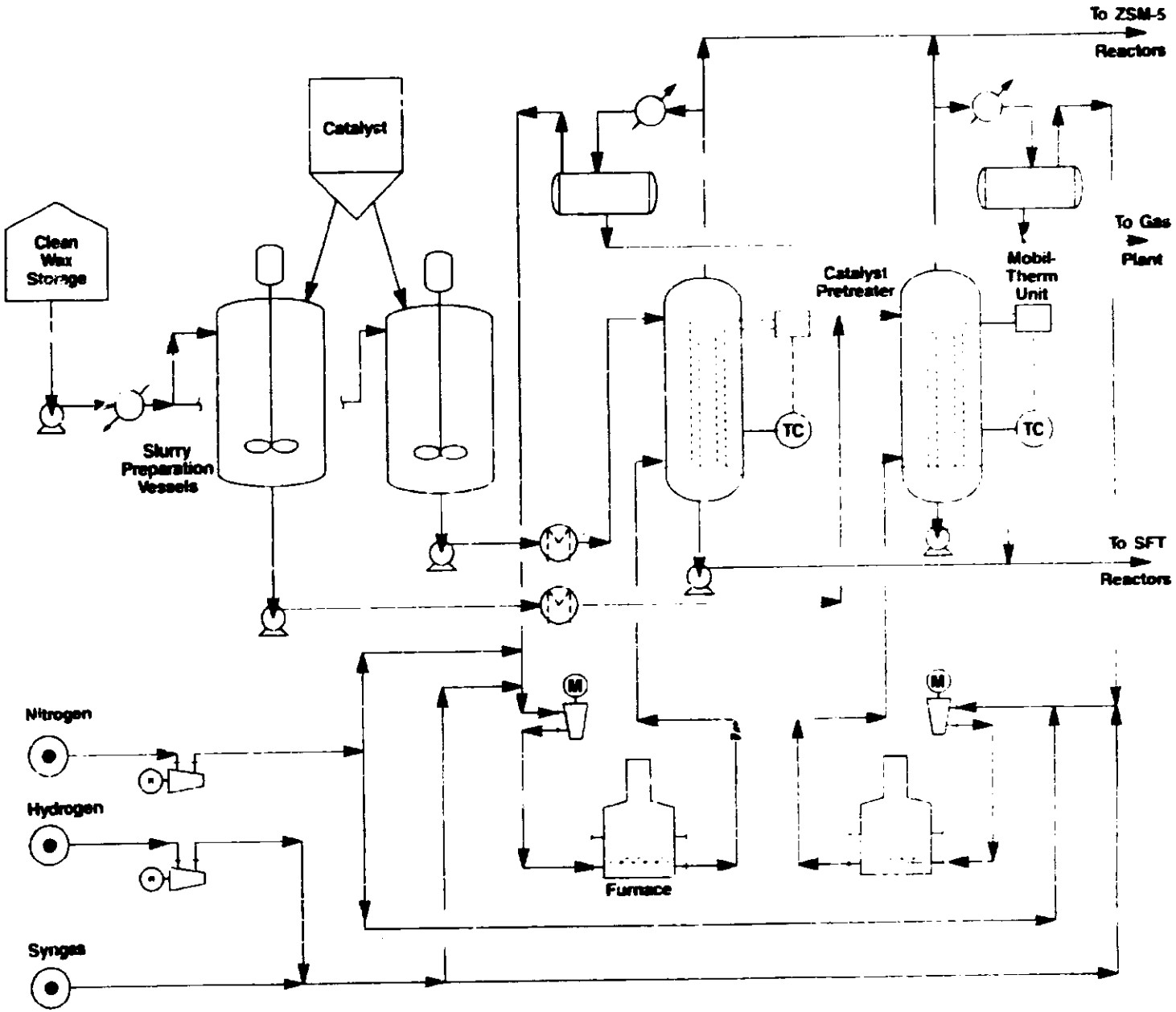

Figure VIII-3
SLURRY FISCHER-TROPSCH/ZSM-5
REACTOR SECTION PLAN

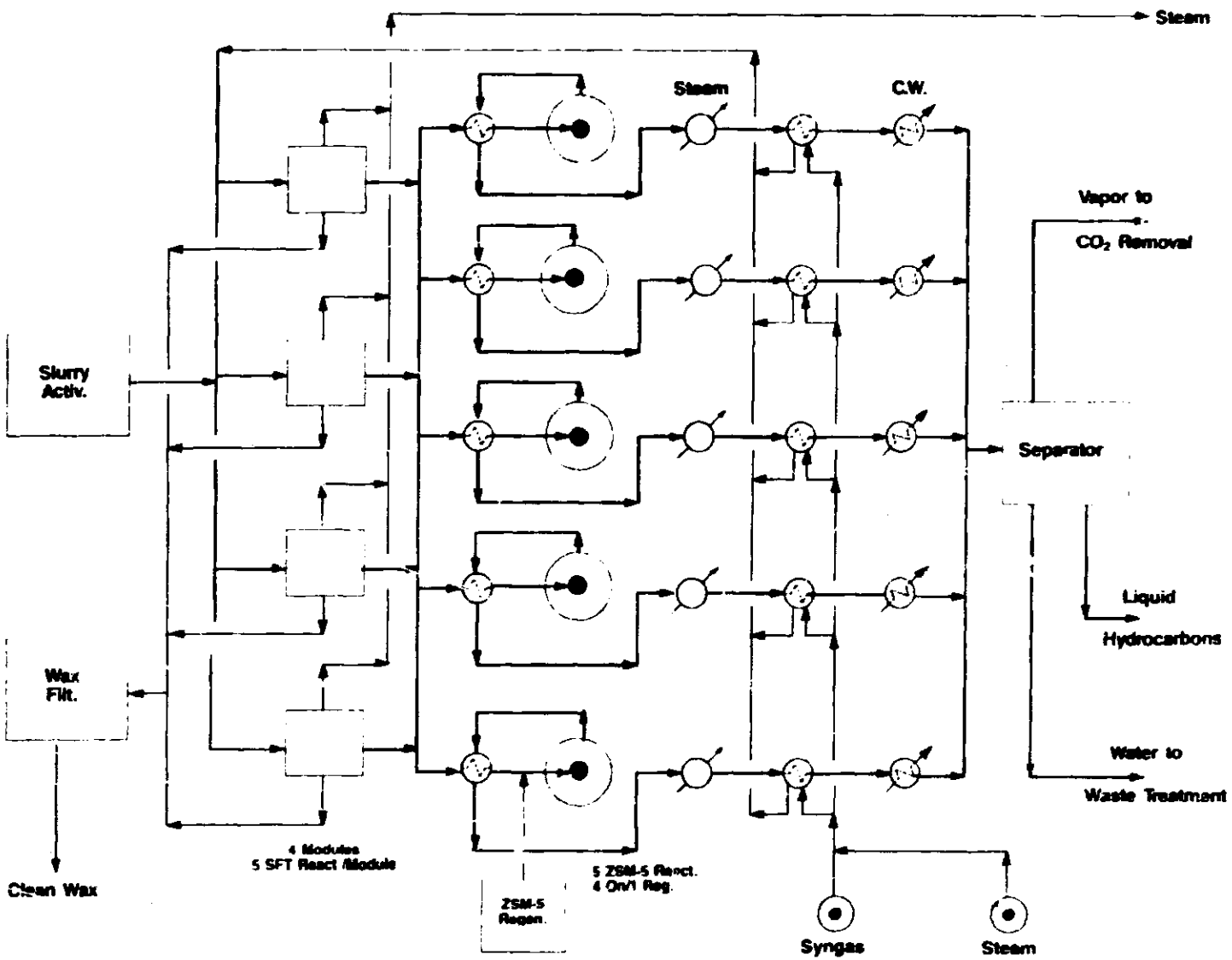

C.2a. Slurry Fischer-Tropsch/ZSM-5 Reactor Section

C.2a-1. Slurry Fischer-Tropsch Reactors

The clean synthesis gas from the coal gasifiers is received at the battery limits at a pressure of 350 psig. To achieve the slurry F-T reactor operating pressure, the gas is compressed to 448 psig using a steam turbine driven compressor located within the battery limits. The compressed gas is then preheated to 440°F by exchanging against the second-stage reactor effluent. Before entering the slurry F-T reactors the synthesis gas is mixed with steam. The steam flow is calculated to produce a H_2/CO ratio of 0.67 (after water-gas shift reaction).

The lower section of the slurry F-T reactor is 14.5 ft ID by 35 ft. tall, the diameter of the upper section is enlarged to 16 ft. and extends for 14 ft. above the slurry level. Total height of the vessel is 49 ft. The design of this large upper section may be overly conservative for the gas-slurry disengagement. However, its impact on the reactor cost is rather small. The major cost of the reactors is their internals, including the heat-transfer tubes, BFW/steam manifold and feed-gas distributor systems. The bottom section contains the steam tubes for the removal of the heat of reaction. These are vertical tubes immersed in the slurry and arranged in a pattern of concentric circles of tubes located at two tubes diameter from each other. Each tube in turn consists of two concentric tubes. The innermost tube brings the saturated water under forced circulation from the steam drum, the return flow is directed upward through the annular space and back to the steam drum. This configuration is similar to the Rheinprussen-Koppers demonstration reactor.

The wax produced in the slurry F-T reactors is removed continuously using level controllers and pumped to the hydroclone system for removal of the catalyst. A minimum of 99.9% of the catalyst in the slurry is recovered and recycled back to the reactor. The clear wax overhead from the hydroclone is sent to the wax clean-up section. During the experimentation with the two-stage BSU a gravity settler vessel using a residence time less than 3.0 hours was utilized for separating the wax from the catalyst achieving less than 0.1 wt % residual catalyst in the wax. This mode of separation may not be practical for a commercial scale plant and although the hydroclone system was not demonstrated in the BSU, improved performance over the gravity settler can be expected from it. The hydroclone system requires considerably less residence time.

To minimize the number of equipment as well as valves and piping, the slurry F-T reactors are grouped in clusters of five that share a single hydroclone system which consists of one slurry pump per reactor plus an enclosed system of a number of (approximately 300, 10 mm ID cyclonetts) parallel manifolded hydroclone separators (from Dorr-Oliver, Inc., Stamford, CT).

C.2a-2. ZSM-5 Reactors

The vapors leaving the slurry F-T reactor at 496°F are preheated to 700°F by exchanging against the effluent stream (738°F) from the ZSM-5 reactors. There are a total of five reactors, four of them are on stream and one is on regeneration at any one time. These are fixed-bed, downflow adiabatic reactors designed for a space velocity of 8.0 NL/gCat-hr.

After preheating the feed, the ZSM-5 reactors effluent is used to generate 355 psig steam and to preheat the feed synthesis gas to 440°F. Further cooling to 110°F is conducted using cooling water. The three phases: vapor, liquid hydrocarbons, liquid water stream are then separated in the separator vessel.

C.2a-3. ZSM-5 Catalyst Regeneration

Due to coke deposition, the ZSM-5 catalyst undergoes deactivation, which requires a progressively higher inlet temperature to maintain the reaction conversion and selectivity. When the inlet temperature reaches the design limit the reactor is taken off line and replaced with another with regenerated catalyst. In preparation for regeneration the reactor is purged with nitrogen and then heated to 700-900°F using hot nitrogen in a closed circuit. Air is added to the recycle regeneration gas to control the oxygen content in the mixture in order to limit the temperature rise in the catalyst.

The regeneration system consists of a gas circulator, a regeneration gas heater exchangers and compressor suction vessel. The cycle between regenerations is assumed thirty days and the regeneration time allowed is three days.

C.2a-4. Slurry Fischer-Tropsch Catalyst Pretreatment

The conversion of the synthesis gas decreases gradually during operation due to deactivation of the catalyst requiring periodic replacement of the slurry. The acceptable level of activity is assumed to last for a period of approximately 60 to 70 days (equivalent to 815-950 gHC/gFe production). At the end of which the hot slurry from the slurry reactor is transferred to a centrifuge in order to remove most of the catalyst in

suspension. The clean wax is then transferred to a surge vessel for later filtration in preparation for upgrading. The reactor is then loaded with fresh slurry which has been prepared in the slurry preparation and pretreatment section. The total hydrocarbon production of the F-T catalyst was assumed earlier for scoping process studies and was not demonstrated under this Contract. The highest production was 350 gHC/gFe established before catalyst settling.

This section consists of two agitated and heated vessels to prepare the mixture of wax with the solid catalyst. The slurry is then transferred to the pretreater, which is a slurry reactor of the same configuration as the one on line except that instead of generating steam in the tubes, a Mobiltherm-600® fluid is circulated to heat or cool the slurry. The activation process is characterized by a gradual increase in CO and H_2 conversion and is conducted at temperatures of 30 to 40°F higher than normal slurry F-T reactor operation. The slurry preparation and activation process lasts approximately 15-20 hours. The fresh slurry is maintained in suspension by recirculating hot nitrogen. Once the temperature of 540°F has been achieved, the nitrogen is replaced with synthesis gas of 0.67 H_2/CO ratio which is prepared by mixing the 0.5 H_2/CO synthesis gas from the coal gasifiers with the pure hydrogen derived from a hydrogen plant. After pretreatment the slurry is immediately transferred to an empty slurry F-T reactor and feeding of the synthesis gas/steam mixture is resumed immediately.

There are two pretreaters in this design with the objective to shorten the slurry replacement time.

Schematic flow diagram of the slurry F-T catalyst pretreatment section is shown in Figure VIII-2.

C.2a-5. Fischer-Trpsch Reactor-Wax Cleanup

The F-T reactor-wax recovered from the slurry F-T reactors is transferred to a wax surge vessel equipped with an agitator and a pump-around heating system to maintain the wax at a temperature of 250-300°F. In addition to the wax from the hydroclones the wax recovered from the deactivated slurry is also processed through the wax cleanup system. From the surge vessel the wax containing less than 0.1 wt % catalyst is filtered through a vertical leaf filter precoated with filter-aid material to remove traces of the F-T catalyst which otherwise may affect the performance of the downstream reactor-wax upgrading units. At the end of the filtration cycle the filter cake is broken loose from the leaf and collected by a screen conveyor system into a cake hopper for disposal. A total of 8 horizontal tank, vertical leaf filters are required for the plant.

C.2b. Product Recovery Section

The product recovery section consists of a conventional distillation train designed to maximize the recovery of C_3 and C_4 hydrocarbons and to produce gasoline and distillate products. A lean oil absorption type gas plant with a sponge oil absorption tower is required. The distillation train consists of a deethanizer absorber, sponge absorption tower, debutanizer and a gasoline splitter. Included in the recovery section are the alkylation and CO_2 removal facilities.

C.2b-1. Distillation Train

The ZSM-5 reactor effluent cooled to 110°F is separated in three phases in the product separation vessel. The liquid water phase is removed to the waste water system while the liquid hydrocarbons phase is pumped to the deethanizer tower. The vapor phase contains light hydrocarbons and most of the CO_2 produced in the F-T reaction. For removal of the CO_2, the potassium carbonate absorption process is used. The carbon dioxide is disposed of to atmosphere and the hydrocarbon vapors are sent to the gas plant where they are combined with the deethanizer overhead accumulator vapor stream, then dried over a zeolites bed and further cooled and refrigerated to -20°F and phase separated. The liquid phase is recycled to blend with the liquid hydrocarbons stream feed from the ZSM-5 product separator and the vapor phase feeds the bottom of the sponge absorber tower.

The overhead vapor from the deethanizer absorber is combined with a light lean oil stream originated in the stabilizer tower then cooled by water and separated. The liquid phase provides the reflux for the deethanizer and the vapor phase is mixed with the hydrocarbon vapor from the CO_2 removal unit as explained above.

The deethanizer bottoms are fed to the stabilizer tower. The bottom stream from the stabilizer provides the light lean oil stream for the deethanizer overhead vapor and also to feed the gasoline splitter tower. The stabilizer overhead liquid constitutes the feed to the HF alkylation unit. The gasoline splitter tower is designed to produce a gasoline in the overhead, while the bottom stream is split to provide the lean oil for the sponge absorber, and the distillate range product which is removed to storage prior cooling. A schematic process flow diagram of the product recovery is shown in Figure VIII-4.

C.2b-2. Alkylation and Gasoline Blending

The yields assumed for the alkylation unit are typical of Mobil experience using the HF alkylation process for C_3/C_4 olefins. The gasoline blending facilities are typical of refinery operations for production of finished gasoline. Pressurization of this gasoline is assumed at 10.0 RVP.

Figure VIII-4
PRODUCT DISTILLATION SECTION

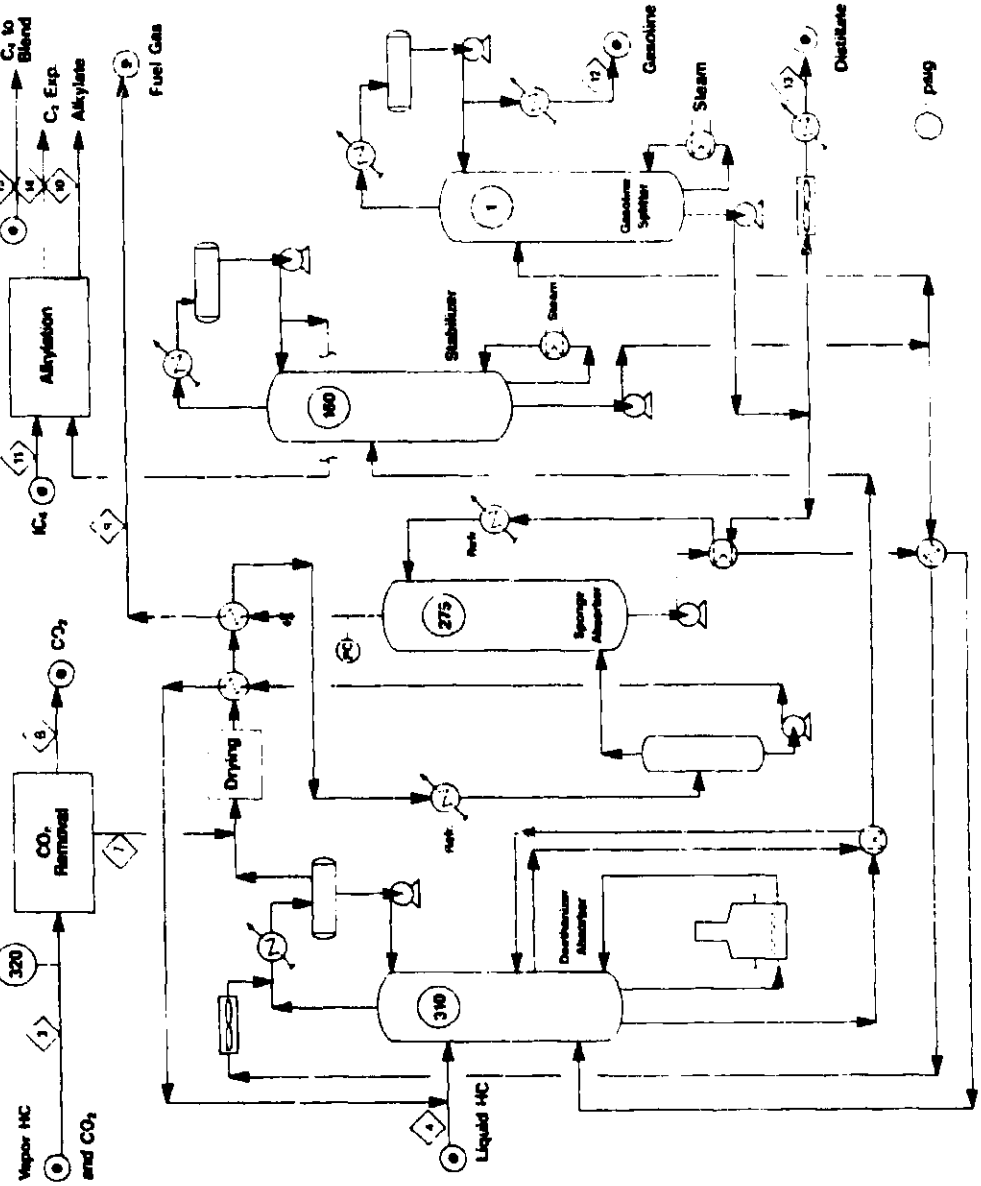

C.2c. List of Major Equipment

Service	No.	Description
Synthesis Gas Compressor	2	Centrifugal Compressor Steam Turbine Driven. 16,000 HP each
Slurry F-T Reactors	22	Bottom Sect. 14.5 ft x 35 ft height. Top. sect. 16.0 ft x 14 ft.
ZSM-5 Reactors	5	15 ft. diam. x 16.5 ft. t-t
Product Separator	1	17 ft. diam. x 20 ft. t-t
Steam Drum (First Stage)	2	11.5 ft. diam. x 49.5 ft. t-t
Steam Drum (Second Stage)	1	4.5 ft. diam. x 19.5 ft. t-t
Wax Surge Vessel	2	14.5 ft. diam. x 50. ft. t-t
Filters Precoat Vessel	1	5.0 ft. diam. x 15 ft. t-t
Horizontal Tank Vertical Leaf Filter	8	Area per Filter 800 $ft.^2$
Centrifuges for Spent Slurry Catalyst Removal	8	Solid Bowl Type-Electric Motor Driven
ZSM-5 Reactor Feed/Effluent Exchanger	5	40 MMBTU/hr each
ZSM-5 Reactor Effl./Steam Generator	5	4 MMBTU/hr each
Synthesis Gas Feed/ZSM-5 Reactor Effluent	5	73 MMBTU/hr each
Fired Heater for F-T Slurry Pretreatment	2	20 MMBTU/hr each
ZSM-5 Reactor Effl./CW	5	12 MMBTU/hr each
Slurry Preparation Vessels	2	13 ft x 45 ft t-t with Electric Motor Agitators

Mobiltherm-600 System (for Slurry Pretreatment)	2	System Includes: Duty. 23 MMBTU/Hr (each) hot oil circulation. Fired Heater, Pumps and Exchangers
Nitrogen/Synthesis Gas Circulator for Slurry Pretreatment	2	Centrifugal Compressor Electric Motor Driven
Nitrogen Booster Compressor	1	Centrifugal Compressor Electric Motor Driven
Hydrogen Booster Compressor	1	Centrigugal Compressor Electric Motor Driven
ZSM-5 Catalyst Regeneration	1	System Includes: Air Compressor, Regeneration Gas Circulation Compressor, Fired Heater
Hydroclones for Wax/Catalyst Separation	4	System Includes Enclosed System of Parallel Manifolded Liquid Cyclones, Circulation Pumps and Strainers
Carbon Dioxide Removal	1	Three Parallel Trains of Potassium Carbonate Absorption and Carbonate Stripper Towers with the Associated Exchangers, Pumps and Knock-Out Drums
Deethanizer Absorber	1	Bottom Section 11 ft. diam. x 100 ft. Top Section 11 ft. diam. x 20 ft. with Fired Reboiler and Overhead Condenser
Sponge Oil Absorber	1	10 ft. diam. x 60 ft. t-t
Stabilizer Tower	1	12.5 ft. diam. x 105 ft. t-t with Steam Reboiler and Water Cooled Overhead Condenser
Gasoline Splitter	1	14.5 ft. diam. x 65 ft. t-t with Steam Reboiler and Water Cooled Overhead Condenser.

C.3. Operating Requirements and Scoping Cost Estimates and Economics

Operating requirements and scoping cost estimates and economics are given in the Appendix-Restrictive Distribution.